(5) S. Alexandratos, "GAUSSIAN-70: The write up" 1976 (QCPE program No. 236)
(6) (a) R. A. Finnegan, *J. Org. Chem.*, **30**, 1333 (1965); (b) A. Streitwieser, Jr., G. R. Ziegler, P. C. Mowery, A. Lewis and R. G. Lawler, *J. Amer. Chem. Soc.*, **90**, 1357 (1968); (c) R. P. Thummel, *Acc. Chem. Res.*, **13**, 70 (1980); (d) R. Homann, *Acc. Chem. Res.*, **4**, 1 (1971).
(7) (a) T. K. Brunck and F. Weinhold, *J. Amer. Chem. Soc.*, **101**, 1700 (1979); *J. Amer. Chem. Soc.*, **98**, 4392 (1976); (b) P. A. Christiansen and W. E. Palke, *Chem. Phys. Lett.*, **31**, 462 (1975); (c) R. Hoffmann, A. Imamura and W. J. Hehre, *J. Amer. Chem. Soc.*, **90**, 1499 (1968). (d) N. D. Epiotis, R. L. Yate's, J. R. Larson, C. R. Kirmaier and F. Bernardi, *J. Amer. Chem. Soc.*, **99**, 8379 (1977).
(8) (a) A. Gavezzotti and L. S. Bartell, *J. Amer. Chem. Soc.*, **101**, 5142 (1979); (b) J. Tyrrell, R. B. Weinstock and F. Weinhold, *Int. J. Quantum Chem. XIX*, 781 (1981).
(9) M. Ohsak, A. Imamura and K. Hirao, *Bull. Chem. Soc. Japan*, **51**, 3443 (1978).

# Superplastic Deformation in the Low Stress Region

**Chun Hag Jang†, Chang Hong Kim and Taikyue Ree**

*Department of Chemistry, Korea Advanced Institute of Science and Technology, P. O. Box 150 Cheongyangni, Seoul 131, Korea* *(Received December 8, 1983)*

**Superplastic alloys generally exhibit a three-stage sigmoidal varition of stress (f) with strain rate ($\dot{s}$), the stages being named region 1, 2 and 3 according to the increasing order of stress or strain rate. In the recent years, two different types of papers have been published on the plastic deformation of Zn-22% Al eutectoid in region I differing in strain-rate sensitivity m ($=d\ln f/d\ln \dot{s}$). In this paper, the data of the two groups have been analysed by applying Kim and Ree's theory of superplastic deformation. (1) We obtained the paramteric values of $X_{gj}/\alpha_{gj}$ and $\beta_{gj}$ ($g$: grain boundary, $j=1,2$ indicating flow units) appearing in Kim and Ree's theory [Eq. (2a)]. (2) It was found that the value of $X_{g2}/\alpha_{g2}$ is small for the group data with small $m$, *i.e.*, $\alpha_{g2}$, which is proportional to the size of flow unit $g2$, is large whereas $\alpha_{g2}$ is small for the groups data with large $m$, *i.e.*, the size of the flow unit $g2$ is small. In other words, the two types of behavior occur by the size difference in the flow units. (3) From the $\beta_{gj}$ value, which is proportional to the relaxation time of flow unit $gj$, the $\Delta H^*_{gj}$ for the flow process was calculated, and found that $\Delta H^*_{g2}$ is large for the group data with small m whereas it is small for the group data with large m. (4) The flow-unit growth was studied, but it was concluded that this effect is not so important for differentiating the two groups.(5) The difference in $\alpha_{g2}$ and in the growth rate of flow units is caused by minute impurities, crystal faults, *etc.*, introduced in the sample preparation.**

## 1. Introduction

Superplastic alloys generally exhibit a three-stage sigmoidal curve in the plot of log $f$ (stress) *vs.* log $\dot{s}$ (strain rate). The Zn–22 % Al eutectoid is one of the best known superplastic alloys, and many studies have been carried out on this alloy.[1~8] Experiments on Zn–22 % Al eutectoid alloys have revealed marked differences in the low stress region 1 so that the published data are divided into two distinct types as shown in Figure 1. In Figure 1 curve A shows a normal sigmoidal type of superplastic deformation,[1,3~6] while curve B does not,[2,7,8] that is, curve B has a higher strain-rate sensitivity ($m=d\ln f/d\ln \dot{s}$) than curve A over the range of low stresses, region 1. In spite of this obvious discrepancy in the strain-rate sensitivity, the two plastic deformations in the low stress region 1 show the same type of flow curves as will be shown later. In this paper much interests are paid on the superplastic deformation in the low stress region 1, and the behavior of superplastic deformation are analyzed according to the Kim-Ree theory.[9] The reason for the appearance of the two different types mentioned above will be clarified.

## 2. Theory

(*a*) *Analysis of Flow Curves.* According to the Ree–Eyring theory,[10~12] the relation between stress and strain rate for dislocation movements are expressed as the following:

$$f=f_d=\sum_{i=1}^{m}\frac{X_{di}}{\alpha_{di}}\sinh^{-1}(\beta_{di}\dot{s}_d) \tag{1a}$$

and

$$\dot{s}_d=\left(\frac{\lambda}{\lambda_1}2k'\right)_{di}\sinh\left[\left(\frac{\lambda\lambda_2\lambda_3}{2kT}\right)_{di}f_{di}\right] \tag{1b}$$

$$=(\beta_{di})^{-1}\sinh(\alpha_{di}f_{di}) \tag{1c}$$

where

$$\alpha_{di}\equiv\left(\frac{\lambda\lambda_2\lambda_3}{2kT}\right)_{di} \tag{1d}$$

and

$$(\beta_{di})^{-1}\equiv\left(\frac{\lambda}{\lambda_1}2k'\right)_{di} \tag{1e}$$

Here, the subscript $d$ represents dislocation, $f$ is the total stress applied on a dislocation slip plane, $f_{di}$ is the stress acting on the $i$th kind of dislocation flow units, $X_{di}$ is the

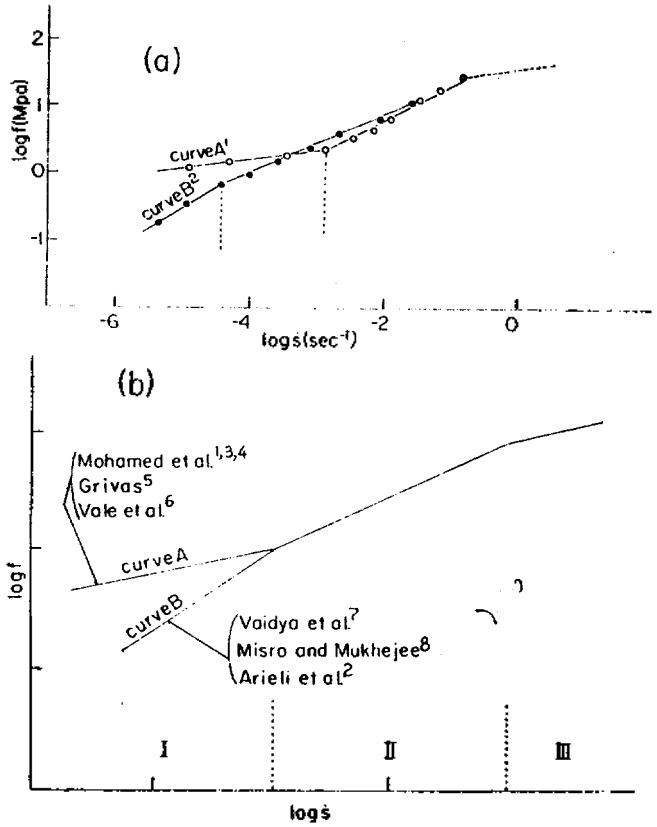


**Figure 1.** log f (stress) *vs.* log ṡ (strain rate) for Zn–22 % Al eutectoid. Figure 1 (a): open circles (curve A) represent Mohamed *et al.*'s data where dashed line indicates schematically the part over the high stress range; filled circles (curve B) represent Mukherjee *et al.*'s data. Figure 1 (b): schematic drawing showing more clearly the difference between curves A and B in Figure 1a. In the figures, reference numbers are shown belonging to the A type and B type curves.

fraction of the area occupied by the $i$ th kind of dislocation flow units, $\lambda_1$, $\lambda_2$, $\lambda_3$ and $\lambda$ are the familar molecular parameters,[10~12] $\alpha_{di}$ and $\beta_{di}$ are flow parameters of flow unit di, and $\beta_{di}$ is a quantity proportional to the relaxation time of the $i$th kind of dislocation flow units, $k'$ being the rate constant for flow. Similar equations for grain-boundary movements can be obtained by changing the subscript $d$ into $g$, which signifys the grain boundary movement, *i.e.*,

$$f=f_g=\sum_{j=1}^{n}\frac{X_{gj}}{\alpha_{gj}}\sinh^{-1}(\beta_{gj}\dot{s}_g) \tag{2a}$$

and

$$\dot{s}_g=\left(\frac{\lambda}{\lambda_1}2k'\right)_{gj}\sinh\left[\left(\frac{\lambda\lambda_2\lambda_3}{2kT}\right)_{gj}f_{gj}\right] \tag{2b}$$

$$=(\beta_{gj})^{-1}\sinh(\alpha_{gj}f_{gj}) \tag{2c}$$

where

$$\alpha_{gj}=\left(\frac{\lambda\lambda_2\lambda_3}{2kT}\right)_{gj} \tag{2d}$$

and

$$(\beta_{gj})^{-1}=\left(\frac{\lambda}{\lambda_1}2k'\right)_{gj} \tag{2e}$$

In Kim and Ree's theory, plastic deformation was dealt with the cases in which the dislocation and grain boundary flows appear simultaneously. The equations derived in Kim and Ree's theory are considered as the generalized equations for plastic deformations of polycrystalline solids, since by various combinations of flow units *di* and *gj* many types of plastic deformation patterns could be described. In Kim and Ree's theory, four cases which are important in practice were presented. For the details of Kim and Ree's theory, reference is made to ref. 9.

According to Kim and Ree's theory, the plastic deformation in the low stress region can be described by two grain boundary flow units which are connected in parallel. For this case, the flow equations are expressed as the following:

$$f=\sum_{j=1}^{2}X_{gj}f_{gj} \tag{3a}$$

and

$$\dot{s}_{gj}=\frac{1}{\beta_{gj}}\sinh\left(\frac{\alpha_{gj}}{X_{gj}}X_{gj}f_{gj}\right) \tag{3b}$$

The plot of $f$ *vs.* $-\ln\dot{s}$ for Eqs. (3a) and (3b) is schematically shown in Figure 2. The broken lines GB1 and GB2 in Figure 2 indicate the curve for flow unit $g1$ and $g2$, respectively, and the solid line is the curve synthesized from GB1 and GB2, *i.e.*, by adding $f_{g1}$ and $f_{g2}$ at a given $\dot{s}$.

In the reverse way, a real flow curve can be analyzed to the curves of GB1 and GB2 as shown graphically, in Figure 2. The flow parameter $X_{gj}/\alpha_{gj}$ ($j=1$ or 2) can be obtained from the slopes of the linear parts of these analyzed curves GB1 and GB2, and the flow parameters $\beta_{gj}$ ($j=1$ or 2) can be calculated from the relation of Eq. (3b) for each analyzed flow curve using the obtained $X_{gj}/\alpha_{gj}$. For the details of the determination of flow parameters reference is made to ref.9.

(*b*) *Calculation of Activation Enthalpies.* According to

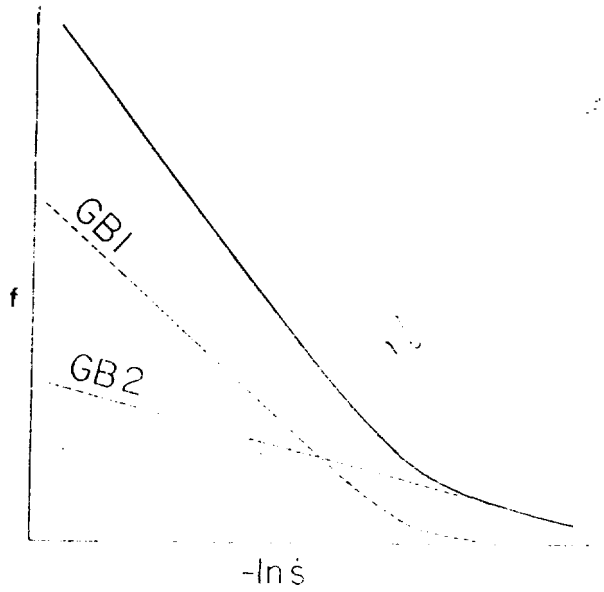


**Figure 2.** Schematic representation of flow curves f vs.– ln $\dot{s}$ for each flow unit. Dotted lines, GB1 and GB2, are the flow curves of grain boundary flow unit $g1$ and $g2$, respectively, and the solid line is the curve synthesized from GB1 and GB2, *i.e.*, by adding f contributed by each unit at a fixed $\dot{s}$.

Eyring's theory,[19] $k'$ in Eq. (2e) can be written as

$$k'=\frac{kT}{h}\exp\frac{\Delta S^*}{R}\exp\left(-\frac{\Delta H^*}{RT}\right) \tag{4a}$$

Introducing this relation to Eq. (2e), one obtains the temperature dependence of $\beta_{gj}$ as the following:

$$\frac{1}{\beta_{gj}}=(\dot{s}_{gj})_0\exp\left(-\frac{\Delta H^*_{gj}}{RT}\right) \tag{4b}$$

where $(\dot{s}_{gj})_0$ is defined as

$$(\dot{s}_{gj})_0\equiv\left[\frac{\lambda}{\lambda_1}\frac{2kT}{h}\exp\left(\frac{\Delta S^*}{R}\right)\right]_{gj} \tag{4c}$$

Here $(\dot{s}_{gj})_0$ can be treated as a temperature independent quantity.[9,14] The $\beta_{gj}$ is also dependent on the grain size. The relationship of $\beta_{gj}$ to grain size has not been completely clarified yet, but many results of studies showed the variation of $\Delta H^*_{gj}$ with grain size, that is, it generally increases with increasing grain size.[15] The variation of $\Delta S^*_{gj}$ with grain size can also be anticipated. But its detailed treatment is omitted here, since the relationship of $\Delta S^*_{gj}$ to grain size is not so important for solving the task to explain the previously mentioned difference in the behavior of plastic deformation as will be clear later [see the part of Theory(d)].

Equation (4b) can be rewritten as the following:

$$\ln\beta_{gj}=\frac{\Delta H^*_{gj}}{R}\cdot 1/T-\ln(\dot{s}_{gj})_0 \tag{5}$$

The plot of $\ln\beta_{gj}$ *vs.* $1/T$ yields a straight line whose slope is $\Delta H^*_{gj}/R$. Thus, the activation enthalpy of the $gj$ flow unit, $\Delta H^*_{gj}$, is obtained from this slope.

(*c*) *Dependence of* $\alpha$ *on the Size of Flow Units.* The flow parameter ($\alpha^{-1}$) is an intrinsic shear stress, and is defined by Eq. (2d), where $\lambda_2$, $\lambda_3$ and $\lambda$ are all proportional to the size of the flow unit. Thus the product $\lambda_2\lambda_3\lambda$ can be written as

$$\lambda\lambda_2\lambda_3=AG^3 \tag{6}$$

where $A$ is a proportionality constant and $G$ is the flow-unit size. As will be shown later, $\alpha$ increases with increasing temperature indicating the growth of flow-units during creep processes. One may assume that the size factor $G$ in Eq. (6) can be expressed by the following equation,

$$G=G'(t-t_0)^p, \tag{7}$$

according to Clark and Alden[16] who used this equation to express the growth rate of *grains* of their samples during experiments. In Eq. (7), $t$ is the time of measurement, $t_0$ is an induction time, $G'$ is the rate of size-growth which is constant under a given strain rate and temperature, and $p$ is a constant. The rate of size-growth $G'$ increases with increasing temperature, and the temperature dependence of the rate of the size-growth can be expressed as:

$$G'=G_0\exp\left(-\frac{\Delta E^*_g}{RT}\right) \tag{8}$$

Here $G_0$ is treated as temperature independent, and it is a constant at a given strain rate, $\Delta E^*_g$ is the activation energy for the size-growth, $T$ is absolute temperature, and $R$ is the gas constant. Here the total volume of the test specimen is assumed to be constant during the size-growth.

Introducing Eqs. (6) to (8) to Eq. (2d), $\alpha$ can be expressed in terms of temperature explicitly as the following:

$$\alpha=\frac{A}{2k}G_0^3(t-t_0)^{3p}\cdot\frac{1}{T}\cdot\exp\left(-\frac{3\Delta E^*_g}{RT}\right) \tag{9}$$

If the time $t$ for measurements of strain rates $\dot{s}$ is kept about equal for a series of experiments, $\alpha$ can further be expressed as a simple function of temperature:

$$\alpha=B\cdot\frac{1}{T}\cdot\exp\left(-\frac{3\Delta E^*_g}{RT}\right) \tag{10}$$

where $B$ is treated as a temperature-independent constant. Equation (10) can be transformed to the following:

$$\ln\alpha T=-\frac{3\Delta E^*_g}{R}\frac{1}{T}+\ln B \tag{11}$$

From Eq. (11), we can expect that the plot of $\ln\alpha T$ *vs.* $1/T$ shows a straight line, and the activation energy of the size-growth $\Delta E^*_g$ can be obtained from the slope of the straight line.

(*d*) *Strain-Rate Sensitivity* ($m$). According to Figure 1, the obvious difference between curves A and B is the difference in strain rate sensitivity (m), that is, curve B has a higher value of $m$ than curve A, which shows a normal sigmoidal type. This higher value of $m$ of curve B is the main interest in the present paper.

Strain-rate sensitivity $m$ is defined as[17]

$$m\equiv\frac{d\ln f}{d\ln\dot{s}} \tag{12}$$

when $m=1$, the flow shows Newtonian behavior, and when $m\geq 0.3$, the flow shows the tendency of superplasticity.[18] In order to calculate the strain-rate sensitivity, the flow equation (2a) is differentiated with respect to $\dot{s}$ as the following:

$$df=\sum_j\frac{X_{gj}}{\alpha_{gj}}\frac{\beta_{gj}\dot{s}}{[1+(\beta_{gj}\dot{s})^2]^{1/2}}\frac{d\dot{s}}{\dot{s}} \tag{13}$$

By a simple manipulation, Eq. (13) is transformed into

$$m\equiv\frac{d\ln f}{d\ln\dot{s}}=\frac{1}{f}\sum_j\frac{X_{gj}}{\alpha_{gj}}\frac{\beta_{gj}\dot{s}}{[1+(\beta_{gj}\dot{s})^2]^{1/2}}=\sum_j m_{gj} \tag{14}$$

Here $m_{gj}$ represents the strain-rate sensitivity of the $j$th grain-boundary flow unit, and is defined as

$$m_{gj}\equiv\frac{1}{f}\frac{X_{gj}}{\alpha_{gj}}\frac{\beta_{gj}\dot{s}}{[1+(\beta_{gj}\dot{s})^2]^{1/2}} \tag{15}$$

When $\beta_{gj}\dot{s}\gg 1$, which is satisfied even at low stress or strain-rate, Eq. (15) can be approximated to

$$m_{g2}\simeq\frac{1}{f}\frac{X_{g2}}{\alpha_{g2}}\simeq m \tag{16}$$

Equation (16) shows that the value of strain-rate sensitivity is related to the flow parameter $X_{g2}/\alpha_{g2}$, since over the range

of low stresses, the flow curve is controlled by the flow unit $g2$ (see Figure 2), *i.e.*, $m \simeq m_{g2}$. The difference in the strain-rate sensitivity over the low stress region of the two group data seems to be due to the difference in the $X_{g2}/\alpha_{g2}$ of the two groups.

## 3. Results and Discussion

(*a*) *The Analysis of Flow Curves.* As mentioned previously, in the low stress region, the flow data for Zn–22 % Al eutectoids can be divided into two distinct groups of curve A and curve B in the plots of $\log f$ *vs.* $\log \dot{s}$ as shown in Figure 1. The experimental data from Mohamed *et al.*'s group[1,3-6] showed normal plastic deformation like curve *A*, and those from Mukherjee et al.'s group[2,7,8] showed plastic deformation like curve B with steeper strain-rate sensitivity at low stresses. The parametric values of $X_{gj}/\alpha_{gj}$ and $\beta_{gj}$ obtained by the analysis of the data of Mohamed *et al.*[1,4] are shown in Table 1, and the parametric values obtained from Mukherjee *et al.*'s experiment[2] are shown in Table 2. The flow curves calculated from Eqs. (3a) and (3b) with the parametric values in Tables 1 and 2 are shown in Figures 3 and 4, respectively. One notes that experimental data are in good agreement with theoretical curves. The theoretical curves in Figures 3 and 4 show the same pattern in the plots of $f$ *vs.* $-\ln \dot{s}$. This means that, there are no mechanistic differences in the behavior of plastic deformations.

(*b*) *The Differences in $\Delta H^*$ of the Two Groups.* In order to study the reason for the distinct difference in the two group data, we shall scrutinize the flow parameters $\alpha$ and $\beta$ more in detail. Flow paramert $\beta$ is a material constant proportional

**TABLE 1: Flow Parameters for Zn–22 % Al Eutectoids. Parameters $X_{gj}/\alpha_{gj}$ and $\beta_{gj}$ were Obtained from Mohamed and Langdon's Experimental data[1,4]**

| Grain size | $X_{g1}/\alpha_{g1}$(Mpa) | $X_{g2}/\alpha_{g2}$(Mpa) | $\beta_{g1}$(sec) | $\beta_{g2}$(sec) | Temp. (K) |
|---|---|---|---|---|---|
| 2.3 $\mu$m | 1.86 | 0.30 | $6.54\cdot10^{4}$ | $2.35\cdot10^{8}$ | 409 |
| | 1.79 | 0.27 | $2.41\cdot10^{4}$ | $8.65\cdot10^{7}$ | 433 |
| | 1.64 | 0.26 | $8.12\cdot13^{3}$ | $9.25\cdot10^{6}$ | 463 |
| | 1.48 | 0.18 | $1.86\cdot10^{3}$ | $4.20\cdot10^{6}$ | 503 |
| 2.5 $\mu$m | 1.92 | 0.36 | $1.75\cdot10^{4}$ | $2.84\cdot10^{6}$ | 423 |
| | 1.83 | 0.34 | $2.15\cdot10^{3}$ | $4.13\cdot10^{5}$ | 473 |
| | 1.70 | 0.31 | $8.56\cdot10^{2}$ | $5.73\cdot10^{4}$ | 503 |

**TABLE 2: Flow Parameter for Zn–22 % Al eutectoids. Parameters $X_{gj}/\alpha_{gj}$ and $\beta_{gj}$ were Obtained from Arieli, Yu and Mukherjee's Experimental Data[2]**

| Grain size | $X_{g1}/\alpha_{g1}$(Mpa) | $X_{g2}/\alpha_{g2}$(Mpa) | $\beta_{g1}$(sec) | $\beta_{g2}$(sec) | Temp. (K) |
|---|---|---|---|---|---|
| 1.3 $\mu$m | 1.74 | 0.42 | $9.25\cdot10^{2}$ | $1.13\cdot10^{5}$ | 450 |
| | 1.43 | 0.35 | $3.13\cdot10^{2}$ | $3.72\cdot10^{4}$ | 500 |
| | 0.95 | 0.29 | $2.33\cdot10^{2}$ | $2.15\cdot10^{4}$ | 525 |
| 2.4 $\mu$m | 1.99 | 0.59 | $1.19\cdot10^{3}$ | $2.53\cdot10^{5}$ | 450 |
| | 1.77 | 0.42 | $4.91\cdot10^{2}$ | $5.48\cdot10^{4}$ | 500 |
| | 1.55 | 0.38 | $1.93\cdot10^{2}$ | $3.37\cdot10^{4}$ | 525 |
| 3.7 $\mu$m | 1.62 | 0.51 | $6.12\cdot10^{3}$ | $6.25\cdot10^{5}$ | 450 |
| | 1.89 | 0.46 | $1.46\cdot10^{3}$ | $1.87\cdot10^{5}$ | 500 |
| | 1.56 | 0.47 | $6.19\cdot10^{2}$ | $4.17\cdot10^{4}$ | 525 |

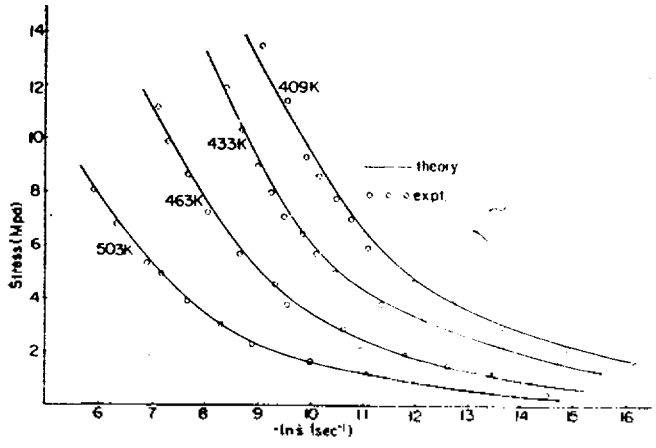


**Figure 3.** Creep curves for Zn–22 % Al eutectoid at various temperatures. The data are from Mohamed *et al.*'s experiments,[4] from which curve A in Figure 1 was drown. Initial grain size was 2.3 $\mu$m.

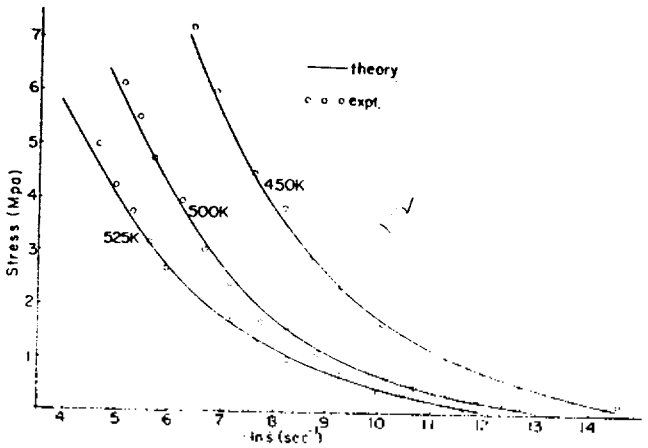


**Figure 4.** Creep curves for Zn–22 % Al eutectoid at various temperatures. The data are from Mukherjee *et al.*'s experiments[2] from which curve B in Figure 1 was drown. Initial grain size was 2.4 $\mu$m.

**TABLE 3: Activation Enthalpies for the Two Types of Zn-22 % Al eutectoids**

| Grain size | Mohamed *et al.*'s sample[1,4] | | | Mukherjee *et al.*'s sample[2] | | |
|---|---|---|---|---|---|---|
| | $\Delta H_{g1}^*$ (kcal/mole) | $\Delta H_{g2}^*$ (kcal/mole) | $\alpha_{g2}/X_{g2}$[a] | $\Delta H_{g1}^*$ (kcal/mole) | $\Delta H_{g2}^*$ (kcal/mole) | $\alpha_{g2}/X_{g2}$[b] |
| 1.3 $\mu$m | | | | 8.8 | 10.3 | 2.86 |
| 2.3 $\mu$m | 15.4 | 18.6 | 5.56 | | | |
| 2.4 $\mu$m | | | | 10.7 | 12.8 | 2.38 |
| 2.5 $\mu$m | 16.1 | 19.9 | 3.23 | | | |
| 3.7 $\mu$m | | | | 13.0 | 13.1 | 2.17 |

[a] The data at 503K from Table 1. [b] The data at 500K from Table 2.

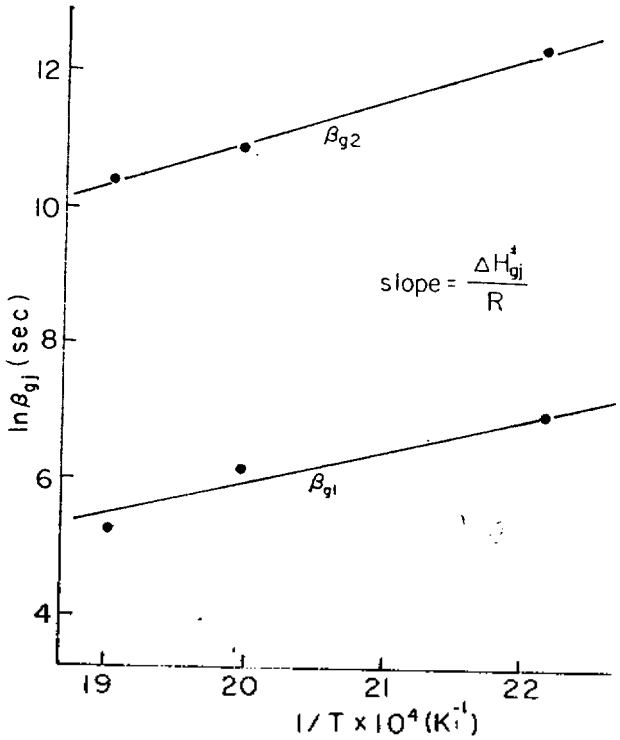


**Figure 5.** Temperature dependence of relaxation times ($\beta_{gj}$, $j$=1 or 2) for Zn-22 % Al eutectoids of Mukherjee *et al.*'s experiment.[2] Data are for the sample of grain size 2.4 $\mu$m in Table 2.

to the relaxation time of flow units in the flow process. By applying the method mentioned in the Theory Part (b), the activation enthalpies were obtained from the $\beta_{gj}$ values in Tables 1 and 2. The plots of $\ln \beta_{gj}$ *vs.* $1/T$ by using the data in Table 2, which were obtained from Mukherjee et al.'s experiment,[2] are shown in Figure 5. Similar plots were obtained by using the data in Table 1, which were obtained from Mohamed *et al.*'s experiment.[1,4] But the plots are not shown here. The $\Delta H_{gj}^*$ values obtained from these plots [see Eq. (5)] are summarized in Table 3 for various grain sizes. Comparing the values of activation enthalpies, one notes that Mohamed *et al.*'s sample[1,4] deforms with a little higher activation enthalpies than Mukherjee *et al.*'s samples.[2]

(*c*) *Consideration on the* $\alpha$ *Values.* The obvious differences between the two groups of experimental data is in the strain-rate sensitivity over the low stress region (refer to Figure 1). The strain-rate sensitivity is expressed by Eq. (14) or by Eq. (15). According to Eq. (15), strain-rate sensitivity $m_{gj}$ is dependent on the flow parameters, $\alpha$ and $\beta$, at a given stress (or strain rate). But the effect of $\alpha$ is stronger than $\beta$ on the strain-rate sensitivity because of the relation $\beta_{gj}\dot{s} \gg 1$.

We compare the value of $X_{g2}/\alpha_{g2}$(=0.31 MPa) obtained from Mohamed et al.'s experiment (grain size 2.5 $\mu$m, temperature 503 K) in Table 1 with that ($X_{g2}/\alpha_{g2}$=0.42 MPa) obtained from Mukherjee *et al.*'s experiment (grain size 2.4 $\mu m$, temperature 500 K) in Table 2. One notes that $X_{g2}/\alpha_{g2}$ (=0.31) value obtained from Mohamed *et al.*'s experiment is smaller than that (=0.42) obtained from Mukherjee *et al.*'s group under similar experimental conditions. Thus, over the range of low stresses, the strain-rate sensitivity $m$ for Mohamed *et al.*'s data is smaller than that for Mukherjee *et al.*'s data according to Eq. (16), *i. e.*, the behavior of curves A and B in Figure 1 is thus explained.

In Table 3, the values of $\alpha_{g2}/X_{g2}$ at 500K (or 503K) are also included which were obtained from Tables 1 and 2. From Table 3, one notes that the relation[15] $\Delta H^* = a + b \ln X$ ($a, b$: constant, $X$: grain size) is well followed. But $\alpha_{g2}/X_{g2}$ decreases with increasing initial grain size of the samples. The reason is not immediately clear. However, by comparing the data of $\alpha_{g2}/X_{g2}$ in columns 4 and 7 of Table 3, one notes that Mohamed *et al.*'s samples have larger flow units than Mukherjee *et al.* 's since $\alpha_{g2} \propto$ size of flow unit [Eq. (2d)], and since $X_{g2}$ is considered to be independent of the size. From the data of $\alpha_{g2}/X_{g2}$ at other temperatures than at 500K in Tables 1 and 2, are obtained similar results, but the details are omitted here. Anyway, it may be concluded that the difference in the strain-rate sensitivity in curves A and B in Figure 1 is caused by the difference in the $\alpha$-factor, *i.e.*, in the flow-unit size.

(*d*) *On the Growth of Flow Units.* From Tables 1 and 2, one notes that the $X_{gj}/\alpha_{gj}$ values decrease with increasing temperature, if $X_{gj}$ is assumed to be temperature independent; it indicates that $\alpha$ increases with increasing temperature; according to Eq. (10). As menthioned in the Theory Part (c), the activation energy for the size-growth $\Delta E_{gj}^*$ can be calculated from the slope of the plot $\ln[(\alpha_{gj}/X_{gj})T]$ *vs.* $1/T$ according to Eq. (11). Figure 6 is the result from the data in Table 2 which were obtained from Mukherjee *et al.*'s experiment.[2] The plots from Mohamed et al. 's experiment[1,4] were performed in a similar way, but the figure was omitted here. The activation energy $\Delta E_{gj}^*$ obtained from the plots are summarized in Table 4 for the two samples.[1,2,4]

Comparing the two different samples of similar grain sizes in Table 4, the $\Delta E_{gj}^*$ of Mukherjee *et al.* 's sample[2] are a little greater than those of Mohamed et al. 's samples.[1,4] The higher values of activation energies for Mukherjee *et*

**TABLE 4: Activation Energies for the Size-Growth of Flow Units for the Two Types of Zn-22 % Al Eutectoids**

| grain size | Mohamed *et al.*'s sample[1,4] | | Mukherjee *et al.*'s sample[2] | |
|---|---|---|---|---|
| | $\Delta E_{\alpha 1}^{*}$ (cal/mole) | $\Delta E_{\alpha 2}^{*}$ (cal/mole) | $\Delta E_{\alpha 1}^{*}$ (cal/mole) | $\Delta E_{\alpha 2}^{*}$ (cal/mole) |
| 1.3 $\mu$m | | | 1211 | 1503 |
| 2.3 $\mu$m | 639 | 788 | | |
| 2.4 $\mu$m | | | 615 | 1001 |
| 2.5 $\mu$m | 506 | 552 | | |
| 3.7 $\mu$m | | | 209 | 378 |

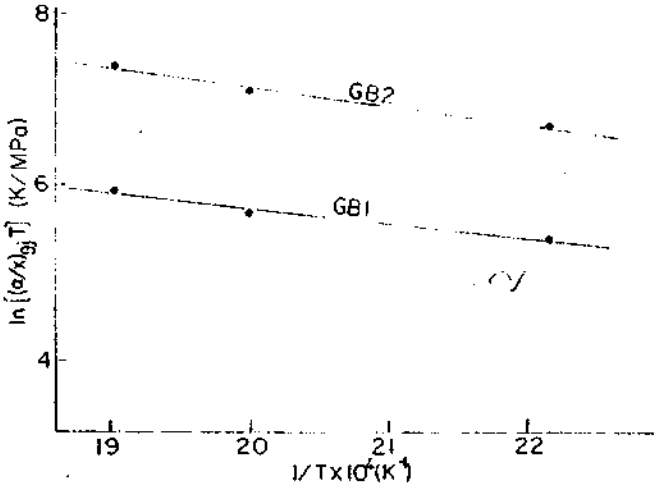


**Figure 6.** Temperature dependence of ln $(\alpha_{gj}/X_{gj})$T for Zn-22 % Al eutectoid of Mukherjee *et al.*'s experiment.[2] Data are for the sample of grain size 2.4 $\mu$m in Table 2.

*al.*'s samples may indicate that the size-growth is slower in the experiment at a given temperature than that for Mohamed *et al.*'s samples. [Note: Since we are not able to estimate $\Delta S_{\alpha}^{*}$ because of the unknown factors involved in the expression for the size-growth process, the above statement is not based on a theoretical basis, but deduced from various experimental results as well as from the $\Delta E_{\alpha j}^{*}$ values.] The difference in the size-growth rate may take a role in differentiating curve A from curve B in Figure 1 besides "the $\alpha$ effect" mentioned above [see the part of Results (c). Curve B stays lower than curve A in Figure 1 because of the difference in the $\alpha$'s, but also by the difference in the growth rates since the slow size-growth rate in curve B makes it stay always lower than curve A in which the rate is faster. But, the growth-rate effect may be considered as a secondary effect. Then the following questions occur about the samples of the two research groups: (1) why the $\alpha$ values are different in spite of the fact that the sample of Zn-22 % Al eutectoid was used by the two groups both, and (2) why the rates of grain-growth are different in the two samples. Both factors, $\alpha$ and size-growth rate, are sensitively influenced by minute impurities, crystal faults, ledges, *etc.* Thus, we belive that these unknown factors have caused the difference in the strain-rate sensitivity over the range of low stresses.

*Acknowledgement.* We acknowledge the Korea Research Center for Theoretical Physics and Chemistry for a partial support of this work.

## References

(1) F. A. Mohamed, M. I. Ahmed and T. G. Langdon, *Met. Trans. A*, **8A**, 933 (1977).
(2) A. Arieli, A. K. S. Yu and A. K. Mukherjee, *Met. Trans. A*, **11A**, 181 (1980).
(3) F. A. Mohamed and Langdon, *Acta Met.*, **23**, 117 (1975).
(4) F. A. Mohamed, S. A. Shei and T. G. Langdon, *Acta Met.*, **23**, 1443 (1975).
(5) D. Grivas, Report No. LBL-7375, Lawrence Berkeley Laboratory, University of California, Berkeley (1978).
(6) S. H. Vale, D. J. Eastgate and P. M. Hazzledine, *Scripta Met.*, **13**, 1157 (1979).
(7) M. L. Vaidya, K. L. Murty and J. E. Dorn, *Acta Met.*, **21**, 1615 (1973).
(8) S. C. Misro and A. K. Mukherjee, "Rate Process in Plastic Deformation of Materials", edited by J. C. M. Li and A. K. Mukherjee, American Society of Metals, Metals Park, Ohio, 1975, p. 434.
(9) C. H. Kim and T. Ree, *J. Korean Chem. Soc.*, **21**, 330 (1977).
(10) F. H. Ree, T. Ree and H. Eyring, *Amer. Soc. Civil Engineers Trans.*, **128**, 1321 (1963).
(11) T. Ree and H. Eyring, *J. Appl. Phys.*, **26**, 793 (1955).
(12) T. Ree and H. Eyring, *J. Appl. Phys.*, **26**, 800 (1955).
(13) H. Eyring, *J. Chem., Phys.*, **4**, 283 (1936).
(14) C. H. Kim and T. Ree, *Bull. Korean Chem. Soc.*, **1**, 39 (1980).
(15) C. H. Kim and T. Ree, *J. Korean Chem. Soc.*, **23**, 217 (1979).
(16) M. A. Clark and T. H. Alden, *Acta Met.*, **21**, 1195 (1973).
(17) J. W. Edington, K. N. Melton and C. P. Cutler, *Progress in Mat. Sci.*, **21**, 67 (1976).
(18) W. A. Backofen, I. R. Turner and D. H. Avery, *Trans. Quart.A.S. M.*, **57**, 980 (1964).